



# A short review article on conjugated polymers

Akhtar Hussain Malik<sup>1</sup> · Faiza Habib<sup>2</sup> · Mohsin Jahan Qazi<sup>3</sup> · Mohd Azhardin Ganayee<sup>4</sup> · Zubair Ahmad<sup>5</sup> · Mudasir A Yattoo<sup>6</sup>

Received: 13 November 2022 / Accepted: 6 January 2023 / Published online: 23 February 2023  
© The Author(s) 2023

## Abstract

This article provides a brief review of conjugated polymers and the various typical polymerization reactions exploited by the community to synthesise different conjugated polyelectrolytes with varied conjugated backbone systems. We further discuss with detailed emphasises the mechanism involved such as photo-induced electron transfer, resonance energy transfer, and intra-molecular charge transfer in the detection or sensing of various analytes. Owing to their excellent photo-physical properties, facile synthesis, ease of functionalization, good biocompatibility, optical stability, high quantum yield, and strong fluorescence emission. Conjugated polymers have been explored for wide applications such as chemical and biological sensors, drug delivery and drug screening, cancer therapeutics and imaging. As such we believe it will be a timely review article for the community.

**Keywords** CPEs · Sensors · PET · RET · FRET · Quencher · Coupling reactions

## General introduction

Conjugated polymers (CPs) are organic macromolecules having alternating  $\sigma$  and  $\pi$  bonds along their backbone. The delocalized  $\pi$ -electron cloud over the backbone chain is responsible for the attractive optical and electrochemical properties of CPs. The conducting nature of CPs was first

discovered [1] and developed by Alan MacDiarmid, Hideki Shirakawa and Alan J. Heeger in 1977 which led them to win the chemistry Nobel Prize in 2000. CPs has attracted significant attention over the last three decades because of their technologically promising future. These CPs have been explored for a variety of applications, including solar cells [2], light emitting diode (LEDs) [3, 4], organic electrochemical transistors (OECTs) [5], energy storage systems [6–8], field-effect transistors (FETs) [9, 10], and chemo- and biosensors [11, 12].

CPs can be acquired with variable backbone chains, viz. poly (p-phenylene) (PPP), poly (p-phenylene vinylene) (PPV), poly (p-phenylene ethynylene) (PPE), polyfluorene (PF), polythiophene (PT), polypyrrole (PPy), etc. as shown in Fig. 1a. Conjugated polyelectrolytes (CPEs) are water-soluble conjugated polymers having pendant ionic functionalities such as sulfonate ( $\text{SO}_3^-$ ), carboxylate ( $\text{CO}_2^-$ ), phosphonate ( $\text{PO}_3^{2-}$ ) and quaternary ammonium ( $\text{NR}_3^+$ ) appended with the main conjugated chain that assists them to ionize in high dielectric media and forming stable electrostatic complexes with target analytes [13–16]. These materials combine the optoelectronic properties of neutral conjugated polymers (CPs) as well as the electrostatic behaviour of polyelectrolytes, thus, providing an exceptional platform in the field of sensors (chemical and biological) [12, 17–19] because of their capability to transform a binding/unbinding event into

✉ Akhtar Hussain Malik  
gmmakhtar@gmail.com

✉ Zubair Ahmad  
Zubair7157@yu.ac.kr

✉ Mudasir A Yattoo  
m.yattoo15@imperial.ac.uk

<sup>1</sup> Government Degree College Sopore, Department of Chemistry, 193201 Jammu and Kashmir, India

<sup>2</sup> Department of Chemistry, University College London, Gordon St, London WC1H 0AJ, UK

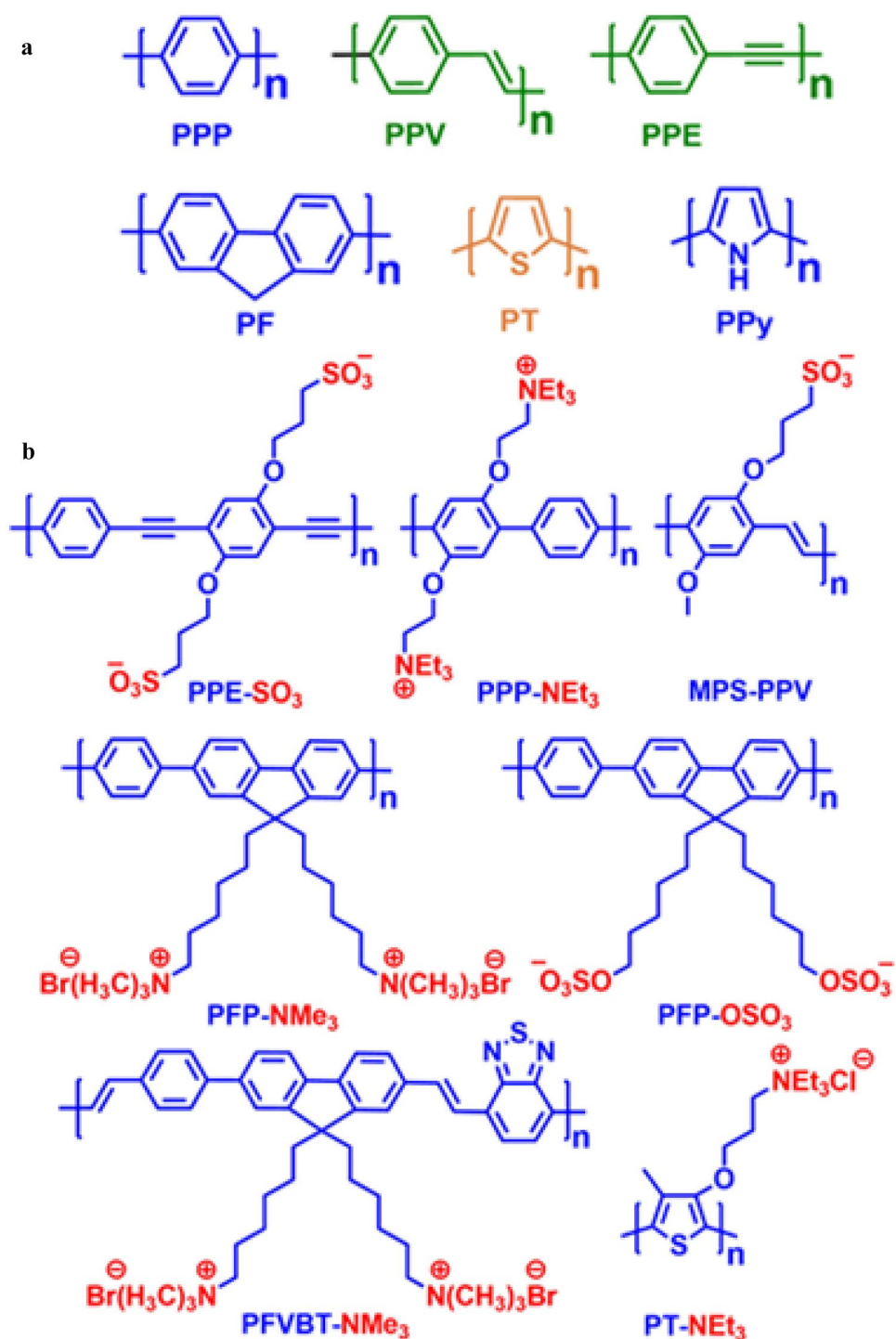
<sup>3</sup> Meining School of Biomedical Engineering, Cornell University, Ithaca, NY 14853, USA

<sup>4</sup> Department of Chemistry, Indian Institute of Technology Madras, 600036 Chennai, India

<sup>5</sup> School of Chemical Engineering, Yengnam University, 38541 Gyeongbuk, Republic of Korea

<sup>6</sup> Department of Materials, Imperial College London, Exhibition Road, London SW7 2AZ, UK

**Fig. 1** Structures of some (a) common conjugated polymer backbones (b) selected examples of conjugated polyelectrolytes



a measurable optical or electrochemical response, excellent biocompatibility, low cytotoxicity, strong emission brightness and resistance to photo-bleaching. Some examples of CPEs are presented in Fig. 1b above.

### Synthesis of conjugated polymers

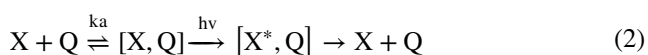
During the past few decades, a large number of CPEs have been designed and synthesised using the same

conjugated backbone structure. Based on the structure of backbone moiety CPs can be classified into various types, namely poly(flourene-co-phenylene) (PFP), poly(p-phenylenevinylene) (PPV), poly(p-phenyleneethynylene) (PPE), polydiacetylenes (PDA), and poly(thiophene) (PT). For the synthesis of various CPEs commonly employed reactions (Suzuki [20], Heck [21], and Sonogashira [22], Wessling reaction [23], photopolymerization reaction [24], and FeCl<sub>3</sub> oxidative polymerization [25]) are shown in Table 1.

### Amplified quenching effects

One of the interesting properties of conjugated polymers is the process of efficient fluorescence quenching at low quencher concentrations, which is referred to as amplified quenching [12, 26]. It was Swager and co-workers in 1995 who for the first time demonstrated this phenomenon [26, 27] of super quenching in polymers via the “molecular-wire effect” which is responsible for its superior sensitivity over small molecule indicators. This signal amplification is an outcome of the ability of the CP to generate exciton (bound electron–hole pair) which migrates efficiently along the conjugated backbone. Because of the efficient charge migration, a single quencher unit bound to the receptor site of the polymer will quench the fluorescence of almost the entire polymer chain leading to the amplified quenching response to a target analyte. This incredible feature of CPs validates its widespread application as chemo- and biosensors, since a very dilute concentration of the analyte is required.

### Stern-volmer fluorescence quenching



$$I_0/I = 1 + k_{sv}[Q] \quad (3)$$

From Eqs. (1) and (2), X\* is an excited-state fluorophore, Q is a quencher molecule, k<sub>q</sub> is the bimolecular quenching rate constant, and k<sub>a</sub> is the association constant for the ground-state complex formation [X, Q].

Equation (3) is known as the Stern-Volmer equation, where I<sub>0</sub> is the fluorescence intensity in absence of a quencher, I is the fluorescence intensity in presence of a quencher, and K<sub>sv</sub> is the Stern–Volmer quenching constant. Fluorescence quenching can take place by two different mechanisms i.e., dynamic (collisional) quenching and static (complex formation) quenching. Dynamic quenching (Eq. (1)) occurs when the excited-state fluorophore encounters the quencher molecule which can facilitate non-radiative transitions to the ground state and the

fluorescence is quenched. Static quenching takes place by binding the quencher molecule to the fluorophore. The excited fluorophore generated is immediately and quantitatively quenched (Eq. (2)). In the case of dynamic quenching, K<sub>sv</sub> = k<sub>q</sub>τ<sub>0</sub>, where τ<sub>0</sub> is the fluorescence lifetime of X\*. The lifetime of the fluorophore in this case is reduced in the presence of a quencher (Fig. 2a). On the other hand, K<sub>sv</sub> = K<sub>a</sub>, if quenching is dominated by the static mechanism and its lifetime remains unaffected in presence of a quencher (Fig. 2b). In both static and dynamic quenching, the Stern–Volmer plots of I<sub>0</sub>/I versus [Q] should be linear as per Eq. (3). However, in most cases, the Stern–Volmer plots show non-linearity (curved graph) which can be explained by various complex processes, such as variation in the association constant with quencher concentration, mixed dynamic and static quenching mechanism, and chromophore aggregation.

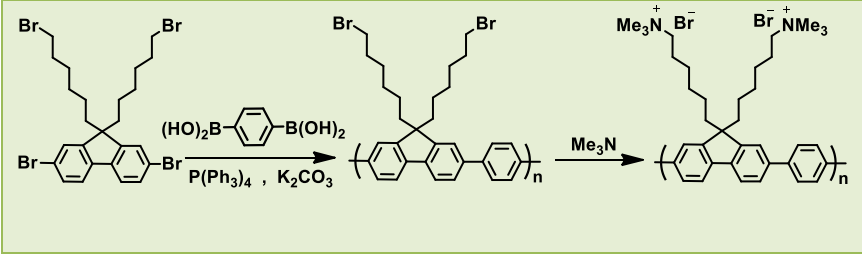
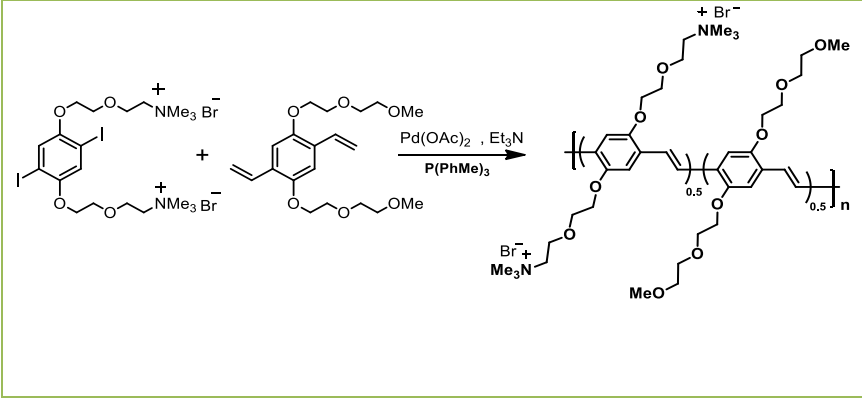
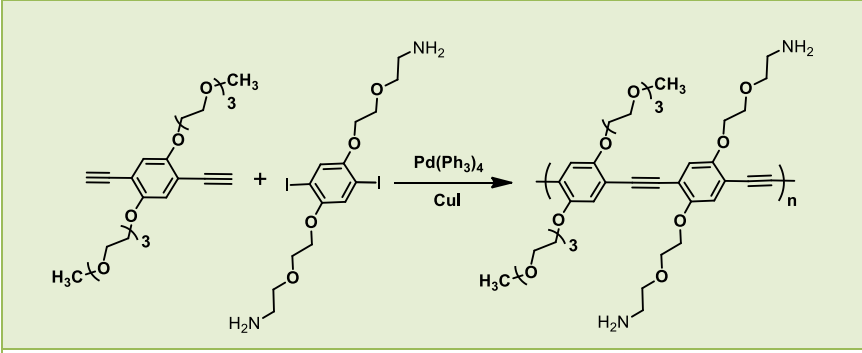
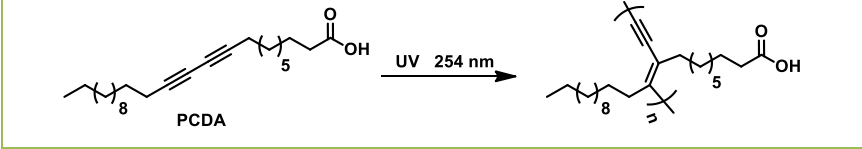
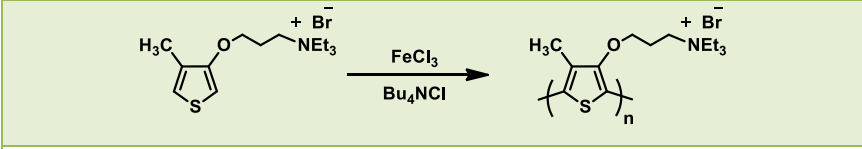
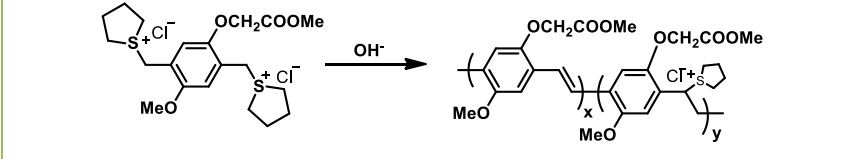
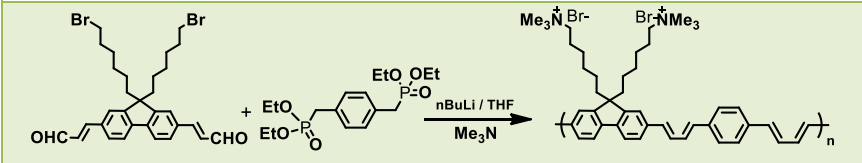
The proposed mechanism of this effect is efficient energy migration along the polymer backbone as discussed above. In 1998 Yang and Swager explored the above phenomena of signal amplification for the sensitive detection of nitro-explosives 2,4,6-trinitrotoluene (TNT) and 2,4-dinitrotoluene (DNT) [28, 29]. However, the super quenching effect in CPEs was first described by Whitten and co-workers in the study of the fluorescence quenching of MPS-PPV by MV<sup>2+</sup> (Fig. 3b) [30]. The fluorescence of the MPS-PPV solution was efficiently quenched by MV<sup>2+</sup>, with a large K<sub>sv</sub> value of 10<sup>7</sup> M<sup>-1</sup>. This amplified quenching was attributed to the strong electrostatic interaction between the negatively charged polymer and MV<sup>2+</sup> which bring them in close proximity resulting in disruption of exciton diffusion along the polymer backbone which leads to efficient fluorescence quenching (Fig. 3a). This study showed that polymer fluorescence is quenched much more efficiently than oligomers.

### Conjugated polymers used as chemo or biosensors

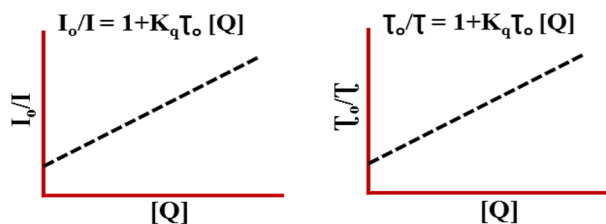
Over the past few decades, CPs have been extensively used as sensory materials for various chemical and biological species [11, 12, 17–19, 31–33] such as metals ions, anions, environmental pollutants, explosive materials, proteins, enzymes, etc. due to their remarkable sensitivity, high photoluminescence quantum yield, large extinction coefficients, photo- and thermal stability, etc. One of the important features of CPs is their capability to transform a binding/unbinding event into a measurable response (electrochemical or optical) which makes them a material of choice for sensing applications.

In general, CP-based fluorescent sensors can operate either in “turn-off” or “turn-on” modes. In the former, the polymer is fluorescent without a quencher, and its fluorescence is turned off upon the addition of the analyte whereas, in the latter, fluorescence is recovered once the quencher is

**Table 1** Common polymerization reactions for the synthesis of CPEs

Schematic Reaction and Structure	Polymerization Method
	Suzuki Coupling (PFP)
	Heck Coupling (PPV)
	Sonogashira Coupling (PPE)
	1,4-Photopolymerization (PDA)
	FeCl <sub>3</sub> Oxidative Polymerization (PT)
	Sulfonium/ Wessling Precursor Route (PPV)
	Witting-Horner Coupling

### a Dynamic Quenching



### b Static Quenching

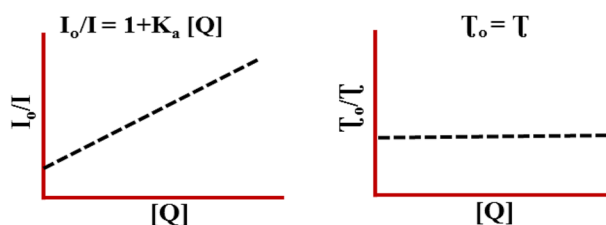


**Fig. 2** Plots showing the effect of quencher concentration on fluorescence emission and fluorescence lifetime in case of **a** Dynamic and **b** Static quenching

added. Most of the CPs work on the principle of non-covalent interaction-based sensing mechanisms such as photo-induced electron transfer (PET), resonance energy transfer (RET), inner filter effect (IFE), and intramolecular charge transfer (ICT) to detect various analytes. In the next subsections, we will discuss the mechanisms in detail.

### Photo-induced electron transfer

In a PET sensing system, complexation takes place between the excited electron donor ( $D^*$ ) and the electron acceptor

species ( $A$ ), here  $D^*$  donates its electron to  $A$  producing a complex  $[D^+ \cdot A^-]$  (Fig. 4i) [34]. Here, the charge transfer (CT) complex relaxes to the ground state via non-radiative transition and the additional electron present on the acceptor can finally return to the electron donor. Thus, PET plays an important role in the process of fluorescence quenching.

### Resonance energy transfer

In RET, acceptor  $A$  absorbs energy from the excited donor  $D^*$  while relaxing to the ground state and getting excited to  $A^*$  (Fig. 4ii). Here, in this case, the rate of energy transfer depends on the relative orientation of the donor and acceptor dipoles, the extent of overlapping of the emission donor and the absorption acceptor, and the distance between the donor and acceptor [12, 35]. Moreover, RET occurs due to the dipolar interaction between the excited donor and acceptor, thus it's not sensitive to steric factors [36, 37].

### Intramolecular charge transfer

In ICT, electron/charge transfer takes place from electron-rich moiety to electron-deficient located in the same molecule. ICT primarily takes place in the photo-excited state of the molecule which facilitates electron transfer from one part of the molecule to another in the excited state. Generally, ICT occurs in those molecules in which donor–acceptor moieties are linked with each other via a  $\pi$ -electron cloud. However, charge transfer can also take place through space but the donor and acceptor must have a favourable orientation.

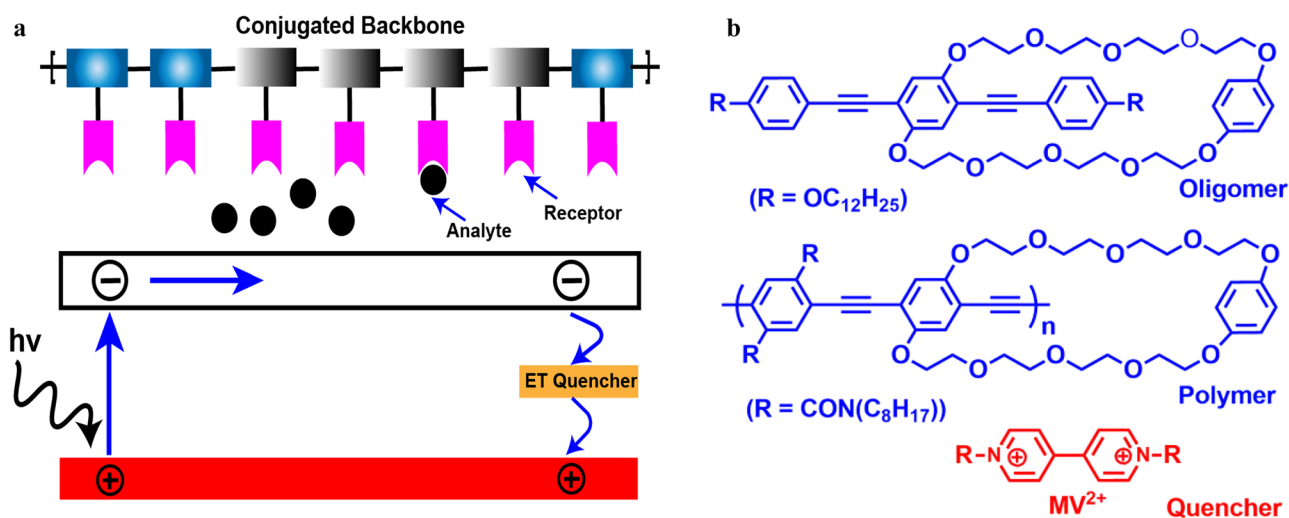


**Fig. 3** **a** Quenching mechanism of molecular wire effect in conjugated polymers **b** structure of oligomer, polymer, and quencher ( $MV^{2+}$ ) used as fluorescence chemosensor for the first time by Swager and co-workers

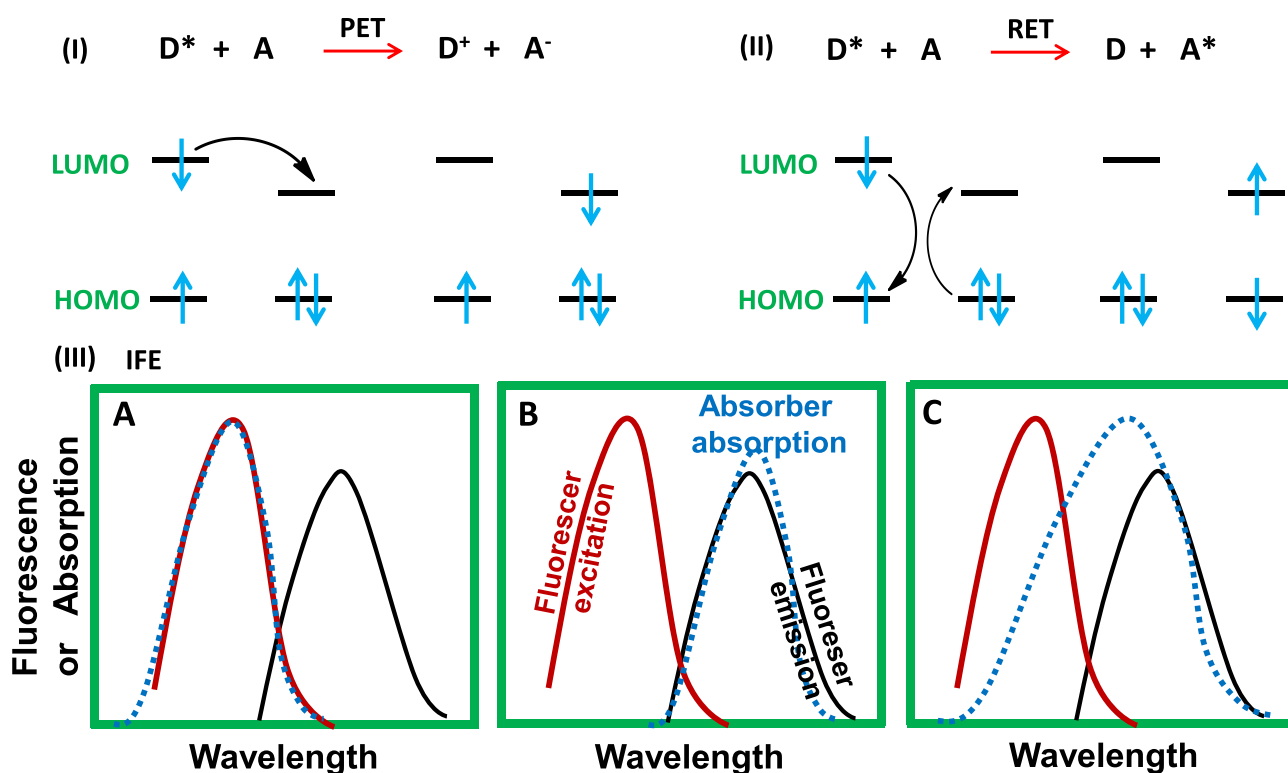


**Fig. 4** Elucidation of the sensing mechanism in conjugated polymers i PET and ii RET iii IFE: **A** absorption spectrum of absorber overlaps with the excitation of fluoreser **B** absorption spectrum of

absorber overlaps with emission spectrum of fluoreser **C** both excitation and emission spectrum of fluoreser overlaps with absorption spectra of absorber

### Inner filter effect (IFE)

IFE was observed by Stokes [38]. It's an important energy conversion model (non-irradiation), resulting from absorption of the excitation or emission light by the absorber [39]. Earlier IFE was considered a problem in fluorescence measurements especially when the analyte with absorbing nature was titrated [40]. In recent years, IFE has emerged as a superior technique in the field of sensing. Two optical units (absorber and fluoreser) are required for the establishment of an IFE based sensing system and for excellent results following points are to be considered. (a) There should be sufficient overlap between the absorption spectrum of absorber and the excitation/emission spectrum of fluoreser. (b) For quantitative analysis of analyte, the absorption spectra of absorber should be sensitive to the analyte concentration. (c) There should be no influence of external agents on the fluorescence and absorption of fluoreser and absorber respectively. (d) There should not be any effect of analyte on the fluorescence emission of fluoreser. (e) The absorber and fluoreser should exist as charge repulsion pairs in order to avoid fluorescence quenching of the fluoreser. Thus IFE-based system provides a simple and flexible method in the field of analytical detection.

### Detection of explosives

One of the most successful applications of CP sensors is in the detection of electron-deficient nitro-aromatic explosives, especially 2,4,6-trinitrotoluene (TNT), trinitrobenzene (TNB), Picric acid (PA) which are of great current interest in both national security and environmental protection because they are not only explosives but also recognized as toxic pollutants [41]. In 1998, Yang and Swager [28] used a fluorescence quenching transduction mechanism along with the amplifying nature of CPs to design **P1** (Fig. 5) as a highly sensitive material to detect TNT vapour. An important feature of this design is the rigid pentiptycene group, which prevents the chains of polymer from aggregating and displaying solution-like optical properties in thin films, therefore, preventing the quenching interaction that can hinder the exciton migration. Polymer **P1** was able to detect TNT at a concentration of 10 ppb after a few seconds of exposure, thus exhibiting extraordinarily high sensitivity because of energy migration through polymer films.

It has been observed mostly that PA exhibits higher quenching efficiencies than TNT because of its lower LUMO energy level. Therefore, detecting TNT in presence of PA in an aqueous solution is challenging. In this regard, Xu et al. [42] in 2011, designed donor-acceptor (**P2**) and donor-only



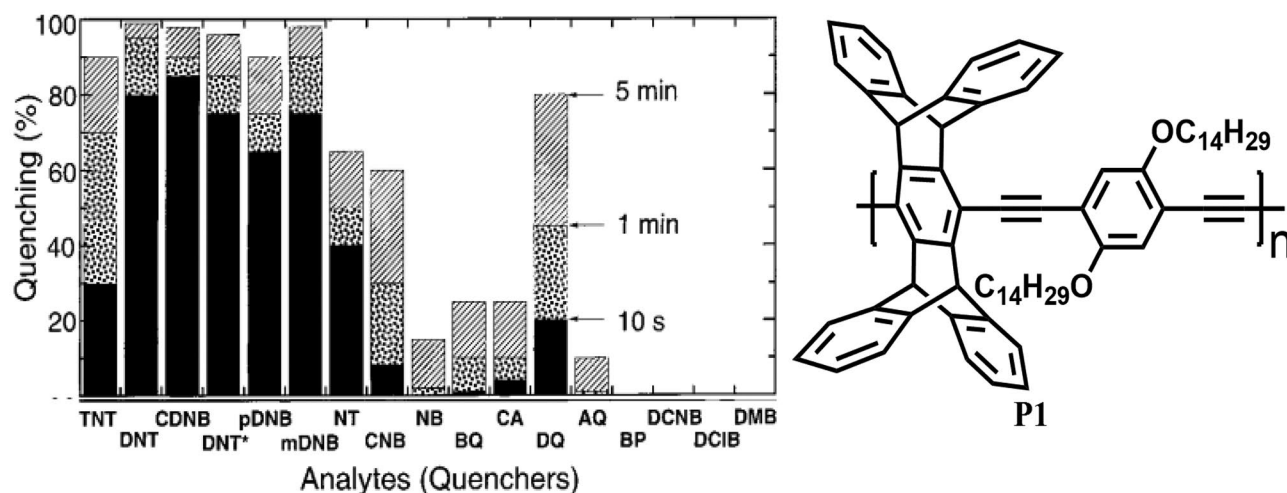


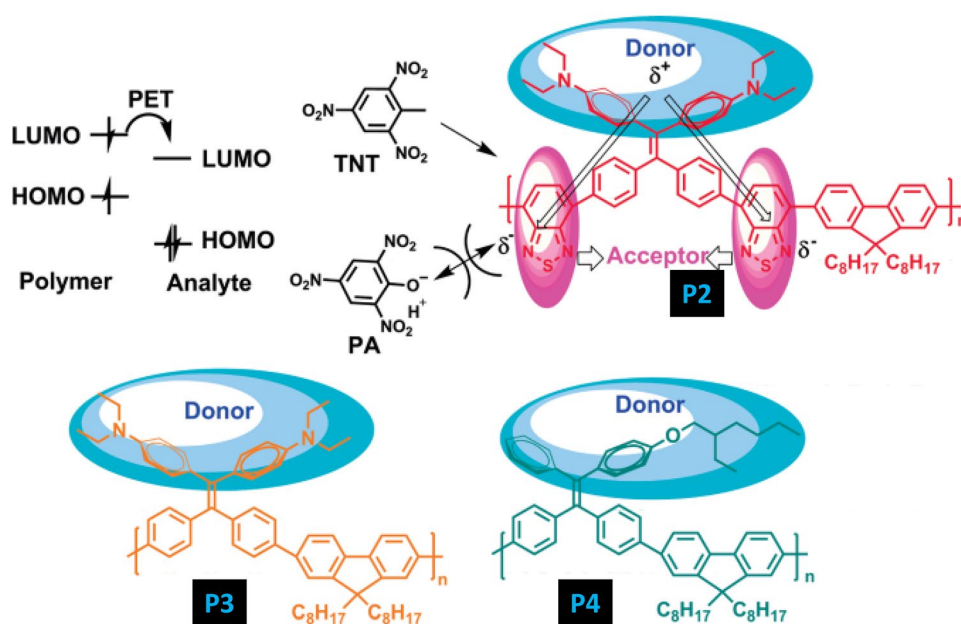
**Fig. 5** Quenching response of CP P1 (pentiptycene derivative) towards vapours of different nitroaromatic analytes including TNT. (The figure is reproduced with permission from Yang and Swager [28] Copyright © 1998, American Chemical Society)

(**P3** and **P4**) AIE active conjugated polymers (Fig. 6) for the selective detection and discrimination of TNT and PA in aqueous solution. In **P2** the LUMO is mainly localized on the acceptor unit of the CP i.e., 2,1,3-benzothiadiazole (BT). Since PA can easily form a negatively charged anion in an aqueous solution, an electrostatic repulsive interaction between the BT unit and PA will disrupt the efficient electron transfer from the LUMO of **P2** to PA which will not occur in the case of TNT. Therefore, **P2** can selectively detect TNT instead of PA in an aqueous solution. In the case of polymer **P3** and **P4** having only donor groups behave similarly to most CP sensors i.e., having greater selectivity toward PA rather than TNT. Furthermore, these polymers were spin-coated and then exposed to the vapours of TNT and PA. For **P1** film, the

$K_{sv}$  of TNT ( $1.2 \times 10^5 \text{ M}^{-1}$ ) is almost 100 times more than that of PA ( $1.8 \times 10^3 \text{ M}^{-1}$ ) and the limit of detection for TNT is about 23 ppb, while the emission of the **P4** film was selectively quenched by PA with  $K_{sv}$  constant of  $2.8 \times 10^4 \text{ M}^{-1}$  and the detection limit of 2 ppb was observed. The fluorescence quenching response follows the order of  $\text{DNT} > \text{TNT} > \text{PA}$ , which can be explained on the basis of the differential vapour pressures of these analytes. Higher quenching for DNT can be attributed to its higher vapour pressure and vice versa in the case of PA.

In 2014, Dong et al. [43] synthesized two poly (3,6-carbazole) **P5** and **P6** (Fig. 7) with AIE-active tetraphenylethylene (TPE) on their side chains via nickel-catalysed Yamamoto coupling under microwave heating. The resulting polymers combine the

**Fig. 6** CPs P1, P2 & P3 has been explored for the selective and sensitive detection of PA and TNT in aqueous media. (The figure is reproduced with permission from Xu et al. [42] Copyright © 2011, American Chemical Society)



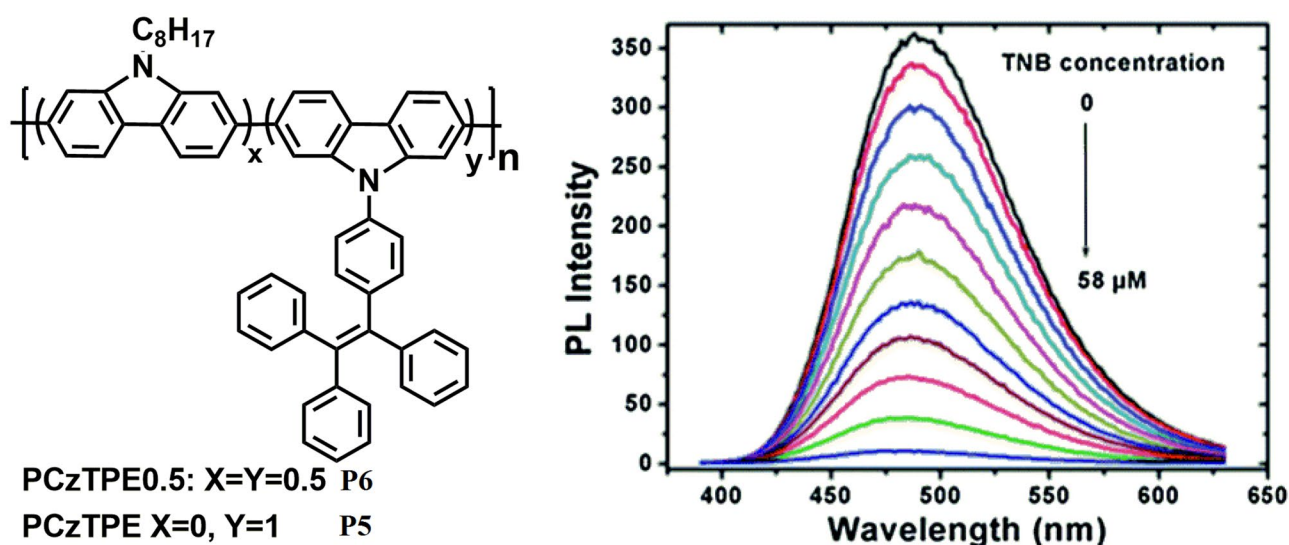


**Fig. 7** AIE active CPs P5 and P6 showed amplified quenching in presence of TNB. (The figure is reproduced with permission from Dong et al. [43] Copyright © 2014, Royal Society of Chemistry)

electron-deficient behaviour of the polycarbazole and the AIE-active nature of TPE and display distinct AIE properties. **P6** shows amplified fluorescence quenching response upon adding trinitrobenzene (TNB) in (1: 9, v/v) THF-water mixtures with a quenching constant of  $1.26 \times 10^6 \text{ M}^{-1}$ . This enhanced quenching is ascribed to the increased number of quenching sites due to the twisted 3D topology of the polymer in the nanoaggregates that can interact with TNB molecules. The mechanism of quenching was deduced to be excited electron transfer from the LUMO of the polymer to the LUMO of TNB.

Furthermore, for practical applications, Whatman filter paper strips were cut and dip-coated into polymer solutions followed by drying in air. Both the polymers show TNB-induced fluorescence quenching in solution as well as in the vapour phase thus demonstrating the potential in solid state sensors for nitroaromatic explosives.

In 2015, Hussain et al. [44] developed a new strategy of introducing an ionic functionality onto the side chain of the polymer as a receptor for the specific interaction of CP with the target analyte. The methyl imidazolium group was introduced into the precursor polymer system to form a cationic polymer **P7** (Fig. 8a). Since PA exists as a negative entity in an aqueous solution and the receptor attached to the CP is positively charged so there is a strong electrostatic attraction which brings the PA in close vicinity resulting in efficient charge transfer or energy transfer from the conjugated polymer to the analyte and ultimately amplified fluorescence quenching is obtained. Here, in this case, the highest quenching constant  $K_{sv}$  of  $1 \times 10^7 \text{ M}^{-1}$  and a detection limit of 128 ppt were obtained which confirms the method to be highly

sensitive towards PA. Furthermore, paper strips and polymer-doped chitosan films were used for the contact mode detection of PA which confirms the method to be practicable. In the same year, Malik et al. [45] developed conjugated polymer nanoparticle (CPN) via re-precipitation technique based on multiple platforms (i.e. 100% water, disposable film and as devices in vapour phase) for the sensing of PA (Fig. 8b). The highest quenching constant ( $K_{sv}$ ) of  $1.12 \times 10^8 \text{ M}^{-1}$  and a very low detection limit of 7.07 ppt was obtained. The reason behind this ultra-sensitivity was electrostatic interaction, photo induced electron transfer (PET) and/or possible resonance energy transfer (RET) between the quencher molecule and the CPN system. The origin of the remarkable selectivity and the exceptional quenching efficiency by PA can be explained via the electrostatic interaction between PA and **P7'**. To investigate the possibility of electron transfer process in the quenching mechanism, HOMO and LUMO levels of **P7'** was obtained and it was found that there is a possibility of excited state electron transfer from LUMO of **P7'** (-3.08 eV) to the LUMO of PA (-3.89 eV) resulting in the quenching process.

### Detection of anions

It is known that selective detection of fluoride anion can be achieved by exploring the unique reactivity of fluoride towards silicon. As shown in Fig. 9a fluoride triggered the removal of silyl from compound **1** which results in the formation of a highly emissive compound **2** (coumarin fluorophore). Kim et al. [46] in 2003 designed polymer **P8** (Fig. 9b) and applied the above strategy for the amplified



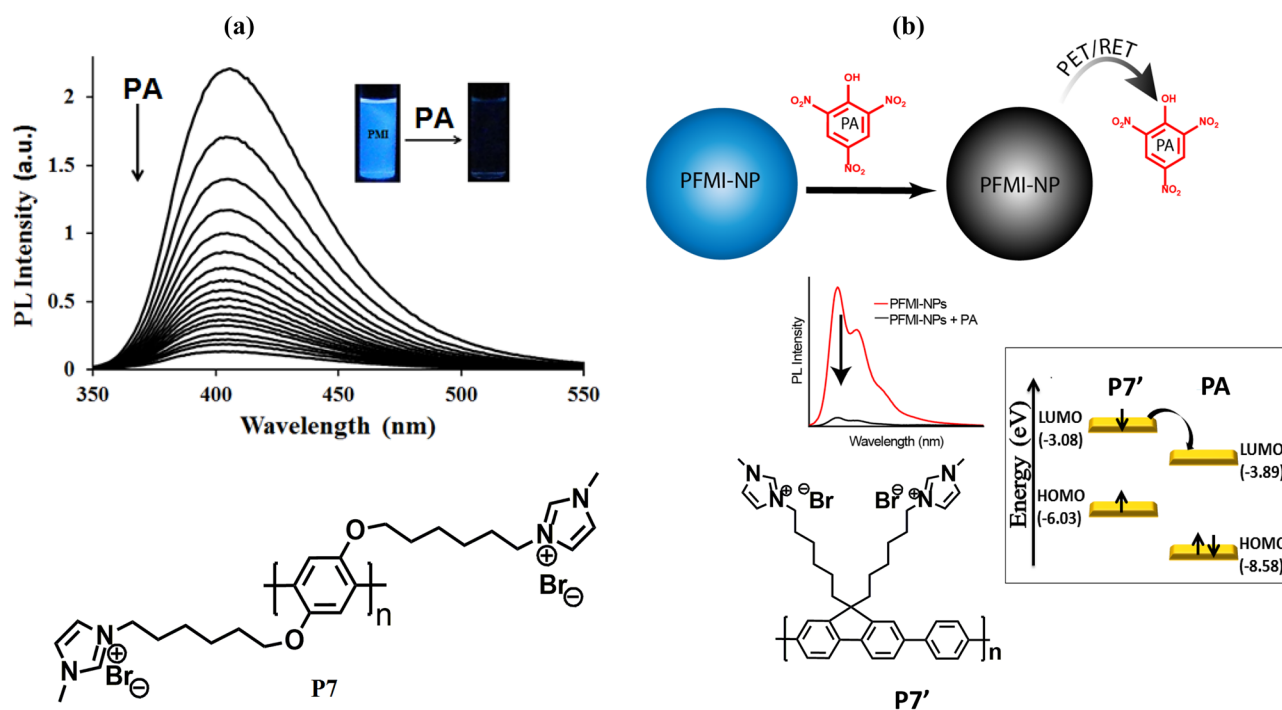


**Fig. 8** **a** Structure of P7 used for PA detection and **b** P7' converting to nanoparticles for the detection of PA on multiple platforms. (The figure is reproduced with permission from Hussain et al. [44] and

Malik et al. [45] Copyright © 2015, Royal Society of Chemistry & Copyright © 2015, American Chemical Society respectively)

detection of fluoride by exploiting the exciton-transporting property of CPs. As anticipated, fluoride-induced formation of coumarin residues along the polymer chain acts as local band gap traps for the migrating excitons and thus gives an enhanced signal response up to 100-fold compared to single molecule-based detection.

In 2010, Zhao and Schanze [47] developed a cationic CPE **P9** (Fig. 10) based on poly (phenylene ethynylene) via Sonogashira coupling reaction with polyamine side chains and explored its application in the ratiometric detection of

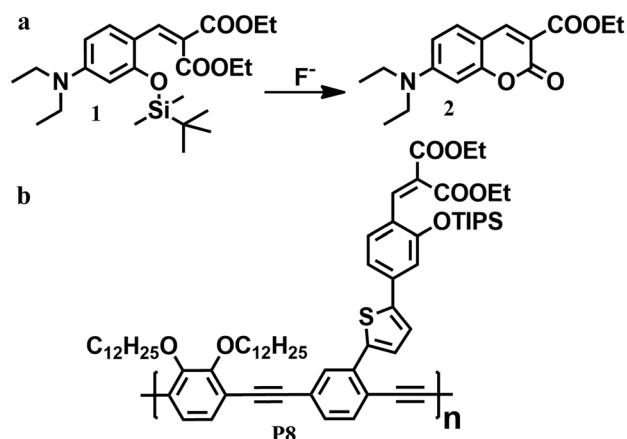
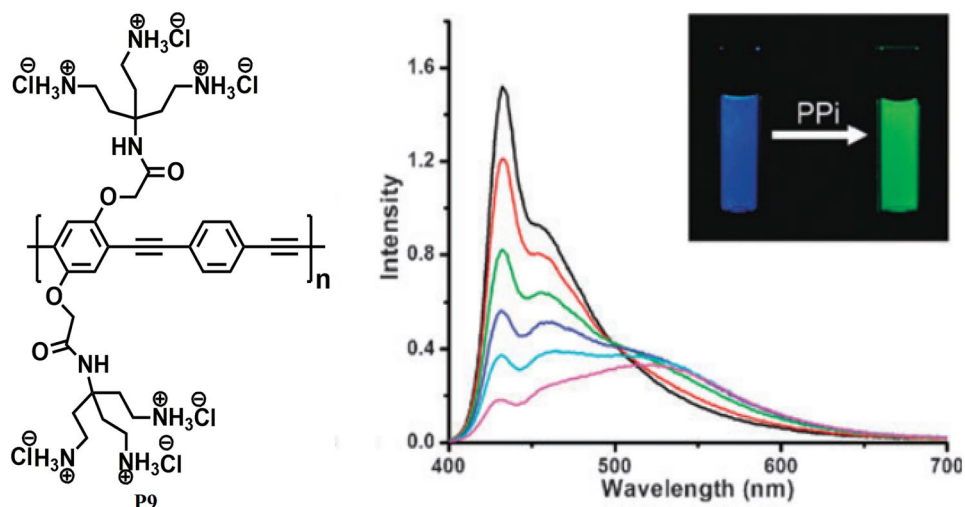


**Fig. 9** **a** Fluoride triggered cleavage of Si–O bond. **b** CP P8 for the detection of fluoride ion via exciton migration

pyrophosphate (PPi) with a detection limit of 340 nM. Polymer **P9** was designed in such a way that it shows redshifts in both emission and absorption spectra upon aggregation. This phenomenon of colour change by switching from the free chain state to the aggregate state was then explored for the naked-eye detection of PPi in an aqueous solution via analyte-induced aggregation of CPE. Upon gradual addition of increasing concentration of PPi into the aqueous solution of **P9**, the absorption band at 400 nm decreases and a new absorption band appear at 430 nm. The emission spectra also reveal the clear transition between the two states as the blue emission with well-resolved peaks between 433–455 nm decreases in intensity with increasing PPi concentration accompanied by an increase in the green emission band at 520 nm. This large red shift of about 90 nm is due to the efficient intermolecular exciton coupling among the polymer chains which results in a lowering of energy in the aggregate state.

In 2011, Wu et al. [48] developed a new CP **P10** (Fig. 11) based on polyfluorene and dicyano-vinyl as a highly selective and sensitive sensor for cyanide. The design of **P10** is based on the fact that the dicyano-vinyl group is a reactive site for cyanide via nucleophilic addition reaction which may disrupt the effective conjugation length of the polymer backbone and perturb its optical properties. Moreover, because of the exciton-diffusing property of CPs along its backbone, the nucleophilic adduct thus formed acts as a charge trapping

**Fig. 10** CP P9 developed for the naked-eye detection of PPI in aqueous solution. (The figure is reproduced with permission from Zhao and Schanze [47] Copyright © 2010, Royal Society Chemistry)



site which may enhance the fluorescence quenching effect and ultimately result in the higher sensitivity of the CP for cyanide ion with a detection limit of 14 ppb.

Furthermore, naked-eye detection of cyanide was also observed upon adding cyanide ions into the polymeric solution as the colour changes from yellow-green to colourless, while no colour change could be observed

in presence of other common anions. In 2012, Evans et al. [49] studied the self-assembly complex formation between the cationic CPE **P11** (Fig. 12) and two anionic surfactants i.e., sodium octyl sulphate (SOS) and potassium heptadecafluoro-1-octanesulfonate (PFOS) both of which are industrially important. The absorption and emission spectra of **P11** were vividly changed in presence of anionic surfactants due to the formation of self-assembly via ionic complex formation. It was observed that subtle structural differences between these surfactants have helped to understand the effect of head group charge density, chain rigidity, and hydrophobicity on both the complex structure and optical properties using UV/vis absorption, fluorescence and Small-Angle Neutron Scattering (SANS). It was concluded that **P11** is capable of identifying anionic surfactants with distinct subgroups via dual-mode detection.

In 2015, Hussain et al. [50] synthesized a new CPE **P7** (Fig. 8a) via oxidative polymerization which displayed high selectivity and sensitivity towards most common anionic surfactants sodium dodecyl sulphate (SDS) and sodium dodecyl benzenesulfonate (SDBS) under various harsh conditions such as full pH range (1–14), urine, and in brine as well as in seawater. Polymer **P7** is very efficient in detecting and discriminating these moderately dissimilar anionic surfactants under acidic and basic conditions with a detection limit of 31.7 and 17.3 ppb respectively for SDBS and SDS in aqueous solution. Furthermore, **P7** could also remove these hazardous surfactants at very low levels from the water and other biological media such as urine in the form of gel or precipitate as a result of its differential aggregation behaviour due to inter-polymer cofacial arrangement via columbic attraction.

In the year 2016, Malik et al. [51] developed **P12** a ratiometric sensor for the naked eye detection of anionic

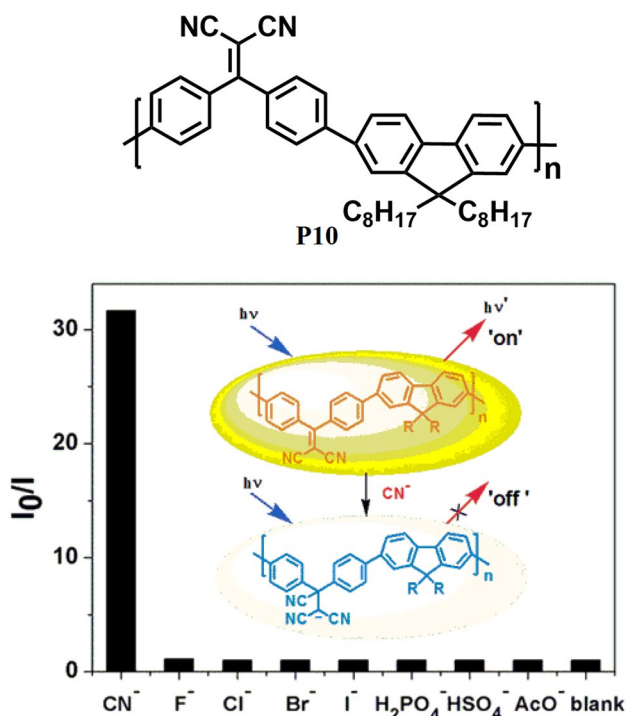
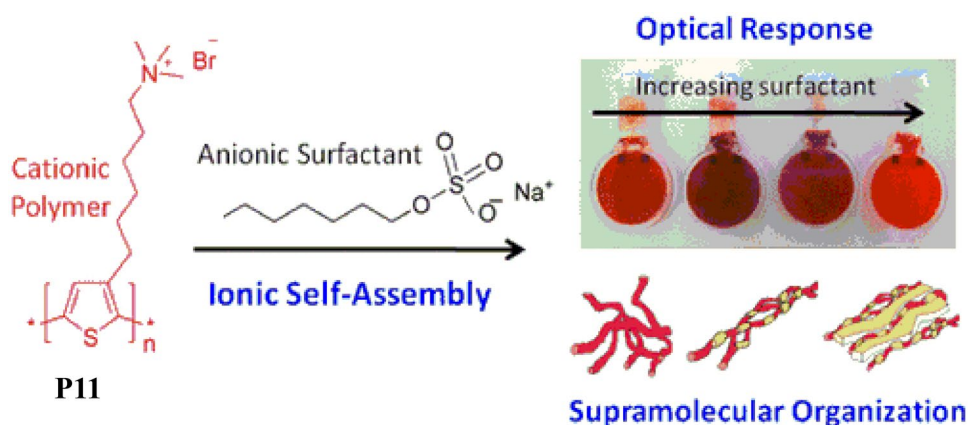


**Fig. 11** Detection of cyanide ion with a detection limit of 14 ppb using CP P10. (The figure is reproduced with permission from Wu et al. [48] Copyright © 2011, American Chemical Society)

**Fig. 12** Structure P11 used for the detection of anionic surfactant. (The figure is reproduced with permission from Evans et al. [49] Copyright © 2012, American Chemical Society)



surfactants such as SDS and SDBS with a detection limit of 34 ppb and 45 ppb respectively in aqueous media. The polymer P12 (PFBT-MI) changed its colour from blue to yellowish green upon interaction with the anionic surfactants which is due to the inter-molecular FRET within the polymer chains driven by electrostatic interaction and hydrophilic interaction between the polymer and the surfactant (Fig. 13).

### Detection of biomolecules

In 2004, Liu and Bazan [52] synthesised a multipurpose cationic CPE **P13** (Fig. 14) via the Suzuki-coupling copolymerization technique by introducing 5% 2,1,3-benzothiadiazole (BT) units into cationic poly(fluorine-co-phenylene) to obtain two distinct emission colours from a single polymer chain. The cationic polymer **P13** strongly

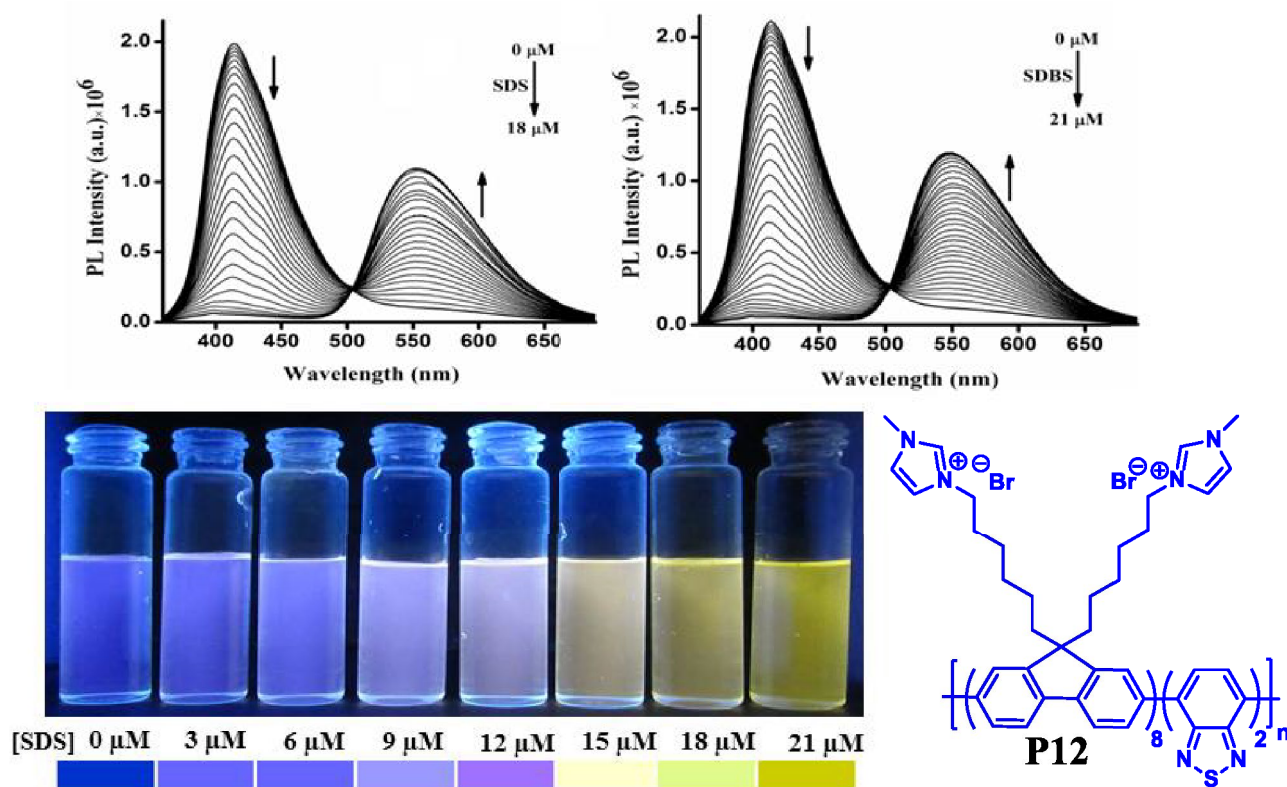


**Fig. 13** Ratiometric sensor for the detection of anionic surfactants SDS and SDBS using CP P12. (The figure is reproduced with permission from Malik et al. [51] Copyright © 2016, American Chemical Society)

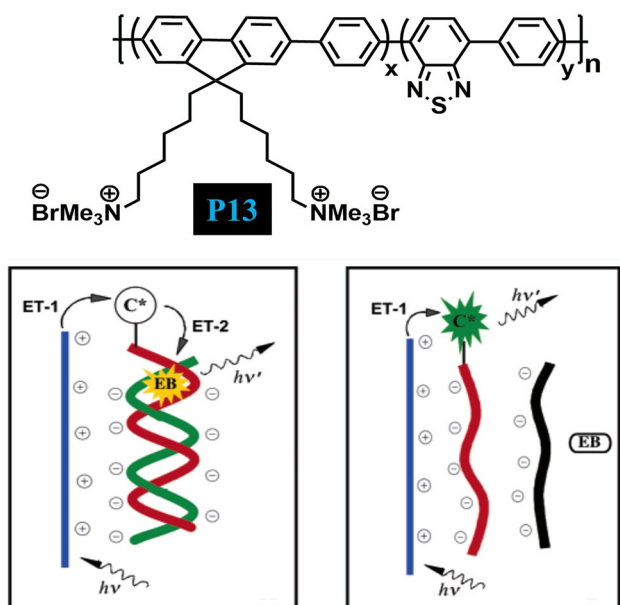


**Fig. 14** CP P13 enabled to determine DNA concentration via the phenomena of FRET. (The figure is reproduced with permission from Liu and Bazan [52] Copyright © 2004, American Chemical Society)

interacts with oppositely charged DNA molecules in an aqueous solution, resulting in the aggregation of polymer chains. Such inter-polymer interactions lead to an increase in the local concentration of benzothiadiazole (BT) units (responsible for FRET) and inter-chain contacts that subsequently improve electronic coupling between the

**Fig. 15** Turn On emission spectra of P14 and P15 for the quantification of heparin via complexation-induced aggregation. (The figure is reproduced with permission from Pu and Liu [53] Copyright © 2009 Wiley-VCH GmbH)

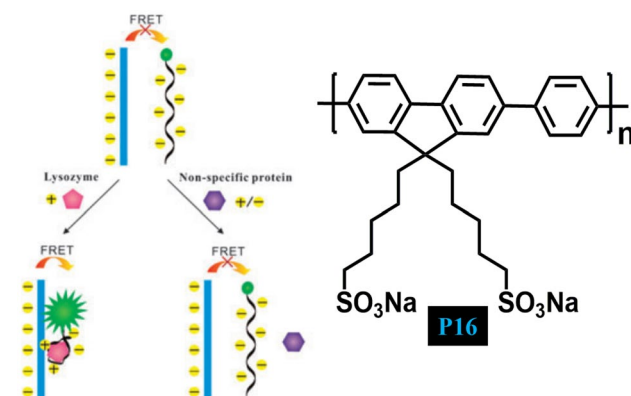
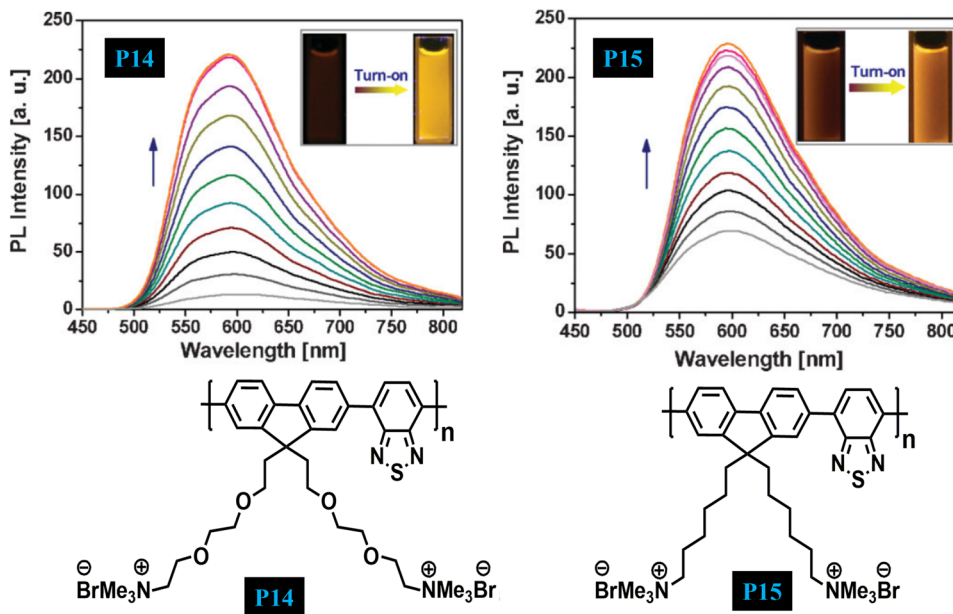
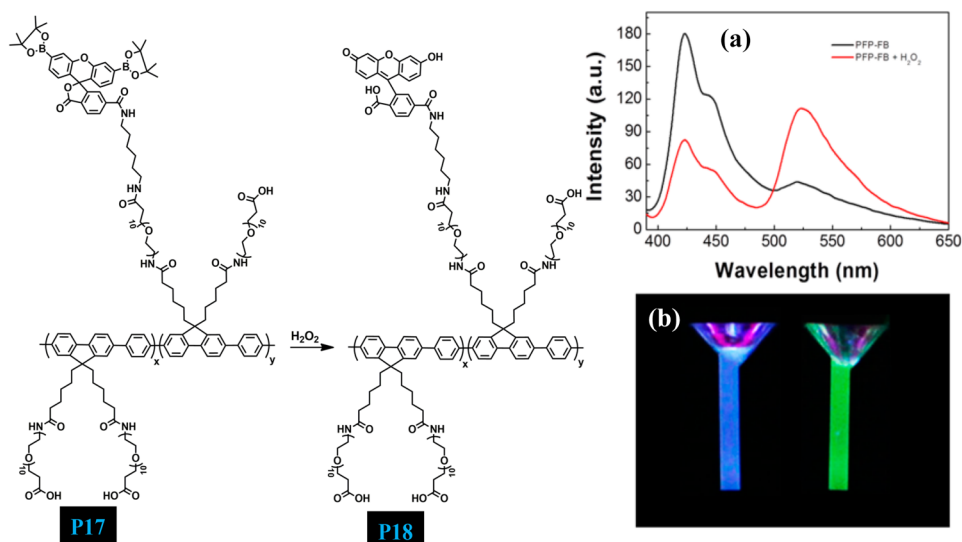


**Fig. 16** CP P16 has been explored for the development of new protein detection strategy via aptamer–target binding to trigger FRET from CP to labelled aptamer. (The figure is reproduced with permission from Wang and Liu [54] Copyright © 2009, Royal Society of Chemistry)

optical partners. This ultimately facilitates the energy transfer process from the fluorine-phenylene (donor) segments to BT (acceptor) units, thus enabling the change in emission colour of the solution from blue to a green that aided in the determination of DNA concentration. Furthermore, the authors demonstrated that polymer **P13** could also be employed as a three-colour DNA assay using a PNA-C\* strand. Depending upon the content of the solution, three different emission colours could be obtained i.e. (i) blue (in the absence of DNA), (ii) green (in the presence of non-complementary ssDNA) and (iii) red (in the presence of



**Fig. 17** **a** PL emission spectra of P17 in the absence and presence of  $H_2O_2$ . **b** Photograph of P17 taken under UV in the absence and presence of  $H_2O_2$ . (The figure is reproduced with permission from Wang et al. [55] Copyright © 2015, American Chemical Society)



complementary ssDNA). Taking advantage of the signal amplification effect of CPs, fine-tuning of electrostatic and optical events leads to multicolour biosensing assay.

In 2009, Pu and Liu [53] designed and synthesized two cationic CPEs **P14** and **P15** which differ only by side chains (Fig. 15). This benzothiadiazole (BT) based CPEs shows low fluorescence emission in an aqueous solution while as its fluorescence increases in the aggregated state. Taking the advantage of complexation-induced aggregation behaviour, a fluorescence turn-on sensor has been developed for the detection and quantification of heparin. A substantial increase in the fluorescence response of the polymer in presence of heparin as compared to its analogue hyaluronic acid (HA) is because of its strong complexation with heparin, thus allowing discrimination of heparin from HA. The advantage of this strategy is that it does not require a pre-quenching

technique and the analyte can be detected directly using this polymer system.

In 2009, Wang and Liu [54] designed a ligand-analyte binding facilitated energy transfer strategy for lysozyme detection using anionic CPE **P16** (Fig. 16) and dye-labelled aptamer. When the lysozyme interacts with the dye-labelled aptamer FRET occurs from **P16** to dye because of the strong electrostatic interactions and green colour formation. In the absence of lysozyme, no FRET happens and the colour of the solution is blue. The simplicity, sensitivity and specificity of this method have been explored by using lysozyme and lysozyme aptamer which has not been observed in other methods like electrochemistry, ELISA, and aptamer assay-based lysozyme assay therefore, this method has been successfully applied in biological media.

In 2015, Wang et al. [55] designed new water-soluble CP **P17** (Fig. 17) with a PEG side chain to which the carboxylic acid group and boronate-protected fluorescein are covalently attached. Carboxylic acid functionality and PEG chain not only increase the solubility of the polymer in water but also reduces nonspecific interactions with the cells and allow further modification of CP (Fig. 18). Efficient fluorescence resonance energy transfer (FRET) takes place from the **P18** backbone to the fluorescein unit in the presence of  $H_2O_2$  upon excitation at 380 nm and the colour of the polymer solution changes from blue to green. Therefore, the polymer probe shows a good ratio-metric fluorescence response to  $H_2O_2$  that was generated from choline and acetylcholine (ACh) under AChE/ChOx enzyme-coupled reaction. The present strategy realizes choline and ACh detection in a simple and selective manner and presents high specificity to choline and ACh, respectively (Table 2).

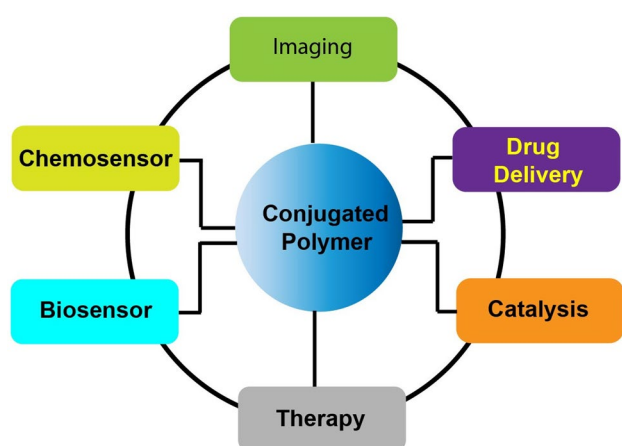


**Fig. 18** Table of content depicting applications of CPs



**Table 2** Various other Conjugated Polymers and their applications

Conjugated Polymer	Excitation	Emission	Sensing Analyte	Sensing Mechanism	Ref
PFEP	405 nm	525 nm	CD44	Disruption of FRET	[56]
PFBT	473 nm	540 nm	Glutathione S-transferase (GST)	Disruption of FRET	[57]
PBEC	430 nm	554 nm	Glutathione (GSH)	Disruption of FRET	[58]
PFO	380 nm	586 nm	Tyrosinase (TR)	Photo-induced electron transfer (PET)	[59]
PFPy	430 nm	553 nm	TNT	RET and FRET	[60]
PFTBTCOOH	380 nm	425 nm	Biogenic amines	Aggregation induced FRET	[61]
PFBT	370 nm	419& 530 nm	Picric acid	IFE	[62]
PF-DBT-PEG	380 nm	420 nm	Thiol	Aggregation induced FRET	[63]
PF-DBTBIMEG	380 nm	420 nm	Adenosine triphosphate (ATP)	Aggregation induced FRET	[64]
PMI	325 nm	406 nm	Nitro-explosive	RET	[44]
PFPBA	410 nm	529 nm	Dopamine	Charge transfer (CT)	[65]
PMI	325 nm	406 nm	Flavins	FRET	[66]
PPE	380 nm	500–580 nm	Imaging of mammalian cells	Electrostatic interaction	[67]
PTPEDC	350 nm	650 nm	in vitro cancer cell-ablation & in vivo zebrafish liver tumor treatment	Photodynamic	[68]
PFMI	370 nm	420 nm	Picric acid	RET	[45]
PPE	380 nm	500 nm	SARS-CoV-2	Photodynamic/electrostatic interaction	[69]

## Conclusions

In this article, recent progress in the design and synthesis of various CPs by exploring various coupling reactions has been summarized. The perspective includes a brief introduction about CPs, followed by a comprehensive study of the sensing mechanism involved. Hence, a new class of materials with exceptional photo-physical properties, good biocompatibility, low cytotoxicity, strong emission brightness and resistance to photobleaching have emerged which resulted in the development of highly selective and sensitive chemical and biological sensors, materials for efficient drug delivery, drug screening, cancer therapeutics, imaging, etc. In conclusion, there is a good potential and opportunity for CPs based approaches to be incorporated into multidisciplinary areas of chemical and biological sciences in the near future.

**Open Access** This article is licensed under a Creative Commons Attribution 4.0 International License, which permits use, sharing, adaptation, distribution and reproduction in any medium or format, as long as you give appropriate credit to the original author(s) and the source, provide a link to the Creative Commons licence, and indicate if changes were made. The images or other third party material in this article are

included in the article's Creative Commons licence, unless indicated otherwise in a credit line to the material. If material is not included in the article's Creative Commons licence and your intended use is not permitted by statutory regulation or exceeds the permitted use, you will need to obtain permission directly from the copyright holder. To view a copy of this licence, visit <http://creativecommons.org/licenses/by/4.0/>.

## References

1. Shirakawa H, Louis EJ, MacDiarmid AG, Chiang CK, Heeger AJ (1977) *J Chem Soc Chem Commun* 578
2. Gunes S, Neugebauer H, Sariciftci NS (2007) *Chem Rev* 107:1324
3. Kraft A, Grimsdale AC, Holmes AB (1998) *Angew Chem Int Ed* 37:402
4. Montali A, Smith P, Weder C (1998) *Synth Met* 97:123
5. Kim JH, Ahmad Z, Kim Y, Kim W, Ahn H, Lee JS, Yoon MH (2020) *Chem Mater* 32:8606
6. Ahmad Z, Lee JS (2022) *Electrochim Acta* 415:140243
7. Kim W, Lee HJ, Yoo SJ, Trinh CK, Ahmad Z, Lee JS (2021) *Nanoscale* 13:5868
8. Ahmad Z, Kim W, Kumar S, Yoon T-H, Lee J-S (2020) *ACS Appl Energy Mater* 3:6743
9. Torsi L, Dodabalapur A, Rothberg LJ, Fung AWP, Katz HE (1996) *Science* 272:1462
10. Sirringhaus H (2005) *Adv Mater* 17:2411

11. McQuade DT, Pullen AE, Swager TM (2000) *Chem Rev* 100:2537
12. Thomas SW, Joly GD, Swager TM (2007) *Chem Rev* 107:1339
13. Jiang H, Taranekar P, Reynolds JR, Schanze KS (2009) *Angew Chem Int Ed* 48:4300
14. Marques AT, Pinto SMA, Monteiro CJP, Melo JSS, Burrows HD, Scherf U, Calvete MJF, Pereira MM (2012) *J Polym Sci Part A Polym Chem* 50:1408
15. Henson ZB, Zhang Y, Nguyen TQ, Seo JH, Bazan GC (2013) *J Am Chem Soc* 135:4163
16. Liu B, Bazan GC (2004) *Chem Mater* 16:4467
17. Zhu C, Liu L, Yang Q, Lv F, Wang S (2012) *Chem Rev* 112:4687
18. Liang J, Li K, Liu B (2013) *Chem Sci* 4:1377
19. Rochat S, Swager TM (2013) *ACS Appl Mater Interfaces* 5:4488
20. Liu B, Wang S, Bazan GC, Mikhailovsky A (2003) *J Am Chem Soc* 125:13306
21. Zhu CL, Yang Q, Liu LB, Wang S (2011) *Chem Commun* 47:5524
22. Moon JH, McDaniel W, MacLean P, Hancock LE (2007) *Angew Chem Int Ed* 46:8223
23. Tang HW, Duan XR, Feng XL, Liu LB, Wang S, Li YL, Zhu DB (2009) *Chem Commun* 6:641
24. Kim JM, Lee JS, Choi H, Sohn D, Ahn DJ (2005) *Macromolecules* 38:9366
25. Ho HA, Boissinot M, Bergeron MG, Corbeil G, Dore K, Boudreau D, Leclerc M (2002) *Angew Chem Int Ed* 41:1548
26. Zhou Q, Swager TM (1995) *J Am Chem Soc* 117:12593
27. Zhou Q, Swager TM (1995) *J Am Chem Soc* 117:7017
28. Yang J-S, Swager TM (1998) *J Am Chem Soc* 120:5321
29. Yang J-S, Swager TM (1998) *J Am Chem Soc* 120:11864
30. Chen LH, McBranch DW, Wang HL, Helgeson R, Wudl F, Whitten DG (1999) *P Natl Acad Sci USA* 96:12287
31. Kim HN, Guo Z, Zhu W, Yoon J, Tian H (2011) *Chem Soc Rev* 40:79
32. Lee K, Povlich LK, Kim J (2010) *Analyst* 135:2179
33. Albert KJ, Lewis NS, Schauer CL, Sotzing GA, Stitzel SE, Vaid TP, Walt DR (2000) *Chem Rev* 100:2595
34. Valeur B (2002) *Molecular fluorescence: Principles and applications*, Wiley-VCH
35. Sun X, Wang Y, Lei Y (2015) *Chem Soc Rev* 44:8019
36. Cantor CR (1980) *Biophysical chemistry: Part II: Techniques for the study of biological structure and function*, Macmillan
37. Zhang Y-Z, Xiang X, Mei P, Dai J, Zhang L-L, Liu Y (2009) *Spectrochim Acta, Part A* 72:907
38. Lakowicz JR (2006) *Principles of Fluorescence Spectroscopy*, 3rd edn. Springer, New York
39. Yuan P, Walt DR (1987) *Anal Chem* 59:2391e2394
40. Parker CA, Rees WT (1962) *Analyst* 87:83e111
41. Tu RY, Liu BH, Wang ZY, Gao DM, Wang F, Fang QL, Zhang ZP (2008) *Anal Chem* 80:3458
42. Xu B, Wu X, Li H, Tong H, Wang L (2011) *Macromolecules* 44:5089
43. Dong W, Fei T, Palma-Cando A, Scherf U (2014) *Polym Chem* 5:4048
44. Hussain S, Malik AH, Afroz MA, Iyer PK (2015) *Chem Commun* 51:7207
45. Malik AH, Hussain S, Kalita A, Iyer PK (2015) *ACS Appl Mater Interfaces* 7:26968
46. Kim T-H, Swager TM (2003) *Angew Chem Int Ed* 42:4803
47. Zhao X, Schanze KS (2010) *Chem Commun* 46:6075
48. Wu X, Xu B, Tong H, Wang L (2011) *Macromolecules* 44:4241
49. Evans RC, Knaapila M, Willis-Fox N, Kraft M, Terry A, Burrows HD, Scherf U (2012) *Langmuir* 28:12348
50. Hussain S, Malik AH, Iyer PK (2015) *ACS Appl Mater Interfaces* 7:3189–3198
51. Malik AH, Hussain S, Iyer PK (2016) *Anal Chem* 88:7358
52. Liu B, Bazan GC (1942) *J Am Chem Soc* 2004:126
53. Pu K-Y, Liu B (2009) *Adv Funct Mater* 19:277
54. Wang J, Liu B (2009) *Chem Commun* 2284
55. Wang Y, Li S, Feng L, Nie C, Liu L, Lv F, Wang S (2015) *ACS Appl Mater Interfaces* 7:24110
56. Huang Y, Zhang X, Ouyang RL, Jiang R, Liu X, Song C, Zhang G, Fan Q, Wang L, Huang W (2014) *ACS Appl Mater Interfaces* 6:19144
57. Han Y, Chen T, Li Y, Chen L, Wei L, Xiao L (2019) *Anal Chem* 91:11146
58. Wang Q-B, Zhang C-J, Lu Q, Liu Z-E, Yao J-S, Zhang X (2020) *Dyes Pigm* 176:108189
59. Sun J, Mei H, Wang S, Gao F (2016) *Anal Chem* 88:7372
60. Tanwar AS, Parui R, Garai R, Chanu MA, Iyer PK (2022) *ACS Meas Sci Au* 21:23
61. Zhong H, Liu C, Ge W, Sun R, Huang F, Wang X (2017) *ACS Appl Mater Interfaces* 9:22875
62. Tanwar AS, Adil LR, Afroz MA, Iyer PK (2018) *ACS Sens* 38:1451
63. Li J, Tian C, Yuan Y, Yang Z, Yin C, Jiang R, Song W, Li X, Lu X, Zhang L, Fan Q, Huang W (2015) *Macromolecules* 48:1017
64. Cui Q, Yang Y, Yao C, Liu R, Li L (2016) *ACS Appl Mater Interfaces* 8:35578
65. Qian CG, Zhu S, Feng PJ, Chen YL, Yu JC, Tang X, Liu Y, Shen QD (2015) *ACS Appl Mater Interfaces* 7:18581
66. Hussain S, Malik AH, Iyer PK (2016) *J Mater Chem B* 4:4439
67. Wang S, Jagadesan P, Sun H, Hu R, Li Z, Huang Y, Liu L, Wang S, Younus M, Schanze K (2020) *S Chem Photo Chem* 5:123
68. Wang S, Wu W, Manghnani P, Xu S, Wang Y, Goh CC, Ng LG, Liu B (2019) *ACS Nano* 13:3095
69. Monge FA, Jagadesan P, Bondu V, Donabedian PL, Ista L, Chi EY, Schanze KS, Whitten DG, Kell AM (2020) *ACS Appl Mater Interfaces* 50:55688

**Publisher's Note** Springer Nature remains neutral with regard to jurisdictional claims in published maps and institutional affiliations.